Antiferromagnetic Spin Fluctuations above the Dome-Shaped and Full-Gap Superconducting States of $LaFeAsO_{1-x}F_x$ Revealed by ^{75}As-Nuclear Quadrupole Resonance

T. Oka,[1] Z. Li,[2] S. Kawasaki,[1] G. F. Chen,[2] N. L. Wang,[2] and Guo-qing Zheng[1,2]

[1]*Department of Physics, Okayama University, Okayama 700-8530, Japan*

[2]*Beijing National Laboratory for Condensed Matter Physics, Institute of Physics, Chinese Academy of Sciences, Beijing 100190, China*

(Received 3 March 2011; revised manuscript received 9 July 2011; published 26 January 2012)

We report a systematic study by ^{75}As nuclear-quadrupole resonance in $LaFeAsO_{1-x}F_x$. The antiferromagnetic spin fluctuation found above the magnetic ordering temperature $T_N = 58$ K for $x = 0.03$ persists in the regime $0.04 \leq x \leq 0.08$, where superconductivity sets in. A dome-shaped x dependence of the superconducting transition temperature T_c is found, with the highest $T_c = 27$ K at $x = 0.06$, which is realized under significant antiferromagnetic spin fluctuation. With increasing x further, the antiferromagnetic spin fluctuation decreases, and so does T_c. These features resemble closely the cuprates $La_{2-x}Sr_xCuO_4$. In $x = 0.06$, the spin-lattice relaxation rate $(1/T_1)$ below T_c decreases exponentially down to $0.13T_c$, which unambiguously indicates that the energy gaps are fully opened. The temperature variation of $1/T_1$ below T_c is rendered nonexponential for other x by impurity scattering.

DOI: 10.1103/PhysRevLett.108.047001 PACS numbers: 74.25.nj, 74.25.Ha, 74.70.Xa

The discovery of superconductivity in $LaFeAsO_{1-x}F_x$ at the transition temperature $T_c = 26$ K [1] has gained much attention in the condensed-matter physics community. The electron doping (F doping) suppresses the antiferromagnetic ordering at $T_N = 140$ K in LaFeAsO, and high-T_c superconductivity appears [1]. The T_c significantly increases up to 55 K in $RFeAsO_{1-x}F_x$ (R: Ce, Pr, Nd, Sm) [2,3]. To elucidate the mechanism of Cooper pairs formation in these arsenides, it is essential to know the superconducting gap symmetry and the normal-state properties. Previous nuclear-magnetic resonance (NMR) and nuclear-quadrupole resonance (NQR) measurements have found that the superconductivity is in the spin-singlet state with multiple gaps [4–6]. Recent systematic measurements on $Ba(Fe_{1-x}Co_x)_2As_2$ [7], $CaFe_2As_2$ under pressure [8], $LaNiAsO_{1-x}F_x$ [9], and $BaFe_2(As_{1-x}P_x)_2$ [10] have suggested that the antiferromagnetic spin fluctuation (AFSF) originated from their multiple electronic bands correlates with the appearance of the pertinent superconducting properties. On the other hand, there are also reports suggesting that AFSF is not important to realize high T_c [11].

For prototypical $LaFeAsO_{1-x}F_x$, several issues remain elusive. One is the role of AFSF. In cuprates, it has been believed that AFSF plays a crucial role to induce high-T_c superconductivity, but the situation in $LaFeAsO_{1-x}F_x$ is still unclear [5,12–16]. Some previous studies by NMR found no AFSF [12–15].

The second issue is the doping dependence of T_c. It was initially reported that T_c forms a wide plateau at $0.04 \leq x \leq 0.12$ [1], which raises a question about the effect of doping. The third unresolved issue is the superconducting gap symmetry. The spin-lattice relaxation rate $(1/T_1)$ decreases sharply below T_c, but the data were insufficient for distinguishing between d-wave from sign-reversal s-wave [5,12–16]. From other experimental probes, some measurements suggested the existence of a node [17], but the photoemission spectroscopy and the point contact Andreev reflection measurement suggested a nodeless gap [18,19].

Here we report results of systematic ^{75}As NQR studies on $LaFeAsO_{1-x}F_x$ ($x = 0.03$, 0.04, 0.06, 0.08, 0.10, and 0.15). An antiferromagnetic order with $T_N = 58$ K is found for $x = 0.03$. Bulk superconductivity sets in at $T_c = 21$ K for $x = 0.04$, with strong AFSF. A dome-shaped x dependence of T_c is found, with the highest $T_c = 27$ K at $x = 0.06$, which is realized under significant AFSF. With further doping, the AFSF is weakened and disappears for $x \geq 0.10$. Concomitantly, T_c decreases. These features resemble closely the case of cuprates $La_{2-x}Sr_xCuO_4$ and suggests that the AFSF is important in producing the superconductivity in $LaFeAsO_{1-x}F_x$ as well. The systematic observation of the AFSF in the low-doping regime is unprecedented, and the high quality samples enable us to reveal a dome shape of the T_c which has a maximum at quite low x. In the superconducting state, $1/T_1$ for $x = 0.06$ decreases *exponentially* down to $0.13T_c$, which is clear and direct evidence for a fully gapped superconducting state. The T variation of $1/T_1$ below T_c is rendered nonexponential for x either smaller or larger than 0.06, showing a seemingly T^3 behavior for $x = 0.10$, which is accounted for by impurity scattering.

The polycrystalline samples of $LaFeAsO_{1-x}F_x$ ($x =$ 0.03, 0.04, 0.06, 0.08, 0.10, and 0.15) were synthesized by the solid state reaction method [20,21]. Here, x indicates the nominal composition of the starting material. Quite often, resistivity measurements give a higher T_c than magnetic susceptibility or NQR. We define T_c by the latter methods. ac susceptibility measurements using

the *in situ* NQR coil indicate $T_c = 21, 27, 23, 18$, and 12 K for $x = 0.04, 0.06, 0.08, 0.10$, and 0.15, respectively. The $1/T_1$ decreases exactly below such-determined T_c. The T_1 is determined by an excellent fit to the single exponential curve $1 - \frac{M(t)}{M_0} = \exp(\frac{-3t}{T_1})$ [21], where M_0 and $M(t)$ are the nuclear magnetization in the thermal equilibrium and at a time t after the saturating pulse, respectively.

Figure 1(a) shows the ^{75}As-NQR spectrum for $0.04 \leq x \leq 0.15$ measured above T_c. As seen in the figure, a clear single peak, which can be fitted by a single Lorentzian curve, is observed for $x \geq 0.06$. The spectra do not change below T_c. However, we observed two peaks for $x = 0.03$ [Fig. 1(b)] and 0.04. This indicates that there are two As sites which are in different surroundings. The NQR frequency ν_Q increases with increasing x, as seen in Fig. 1(c). Here, ν_Q probes the electric-field gradient generated by the carrier distribution and the lattice contribution surrounding the As nucleus. The doping evolution of ν_Q, the spectral shapes, and the single component of T_1 indicate that the electron carriers were homogeneously doped for $x \geq 0.06$, but phase separation occurs in $x = 0.03$ and 0.04. We speculate that this may be due to the local distribution of the F ion around the As nucleus, which is inevitable in a quite low-doping region. Remarkably, the T dependences of $1/T_1$ measured at each peak of $x = 0.03$ and 0.04 indicate that each phase is homogeneous. The same behavior was found in Ref. [22], where the ν_Q is quite similar to ours although the nominal x there is larger than ours by $\sim$0.02 [21]. Figure 1(b) shows the T evolution of the NQR spectra for $x = 0.03$. Below $T_N = 58$ K, the spectra are broadened due to an antiferromagnetic order.

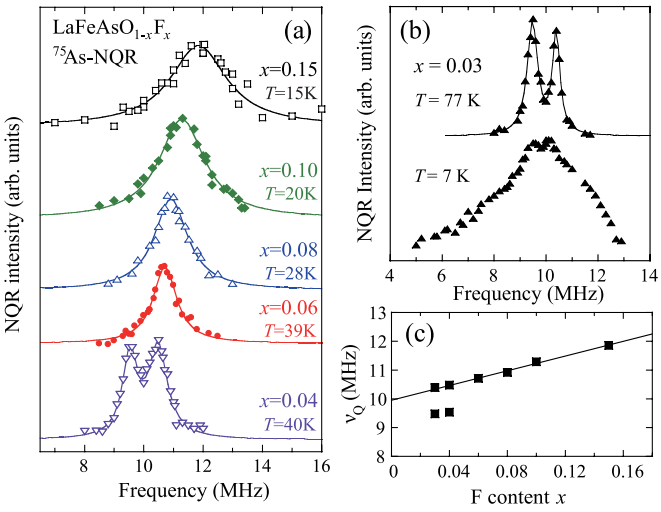

FIG. 1 (color online). (a) Doping dependence of the ^{75}As-NQR spectrum for $LaFeAsO_{1-x}F_x$ measured above T_c. Data for $x = 0.08$ are from Ref. [5]. Solid curves are Lorentzian fittings which give a FWHM of $\sim$0.95, 1.2, 1.8, and 2.3 MHz for $x = 0.06$, 0.08, 0.10, and 0.15, respectively. (b) The spectra above and below $T_N = 58$ K for $x = 0.03$. (c) The x dependence of ν_Q.

Figures 2(a) and 2(b) show the T dependence of $1/T_1$ for all samples. For $x = 0.03$, $1/T_1$ shows a small upturn right above T_N and then decreases below, leaving a tiny peak at T_N. For $x \geq 0.04$, $1/T_1$ decreases rapidly below T_c due to the opening of the superconducting energy gaps.

Before going into the details of the superconducting state, we first discuss the normal-state property. For this purpose, we plot $1/T_1T$ vs T in Fig. 3. None of the samples shows a Korringa relation $1/T_1T = \text{const}$ expected for a conventional metal. Above T_N of $x = 0.03$, $1/T_1T$ increases with decreasing T due to the AFSF. Such AFSF persists in $x = 0.04$, 0.06, and 0.08, where $1/T_1T$ increases with decreasing T down to T_c. To model the $1/T_1T$ above T_N or T_c, we employed the theory for a weakly antiferromagnetically correlated metal [23], $1/T_1T = (1/T_1T)_{\text{AF}} + (1/T_1T)_0 = C/(T + \theta) + (1/T_1T)_0$. Here, the first term described the contribution from the antiferromagnetic wave vector, and the second term is the contribution from the density of states (DOS) at the Fermi level. For $x = 0.03$, θ is simply $-T_N$, where the data can be well fitted except around T_N [24]. As seen in Fig. 3, $1/T_1T$ for $x = 0.04$, 0.06, and 0.08 are well reproduced by this model with $\theta \sim 10$, 25, and 39 K, respectively. The low-frequency NQR peak for $x = 0.04$ gives a smaller

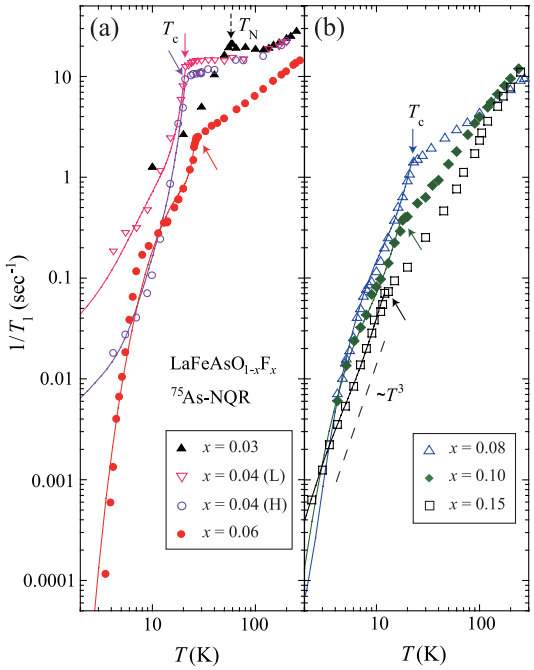

FIG. 2 (color online). The T dependences of $1/T_1$ for $x = 0.03$, 0.04, and 0.06 (a) and for $x = 0.08$, 0.10, and 0.15 (b). Data for $x = 0.03$ were collected at the high-frequency (H) NQR peak. For $x = 0.04$, $1/T_1$ was measured at both the low-frequency (L) and the H peaks. Solid curves below T_c for $x \geq 0.04$ are the simulations based on a $s^{\pm}$ wave superconducting gap model with impurity scattering (see the text). The dashed line indicates the relation $1/T_1 \propto T^3$. The dotted and solid arrows indicate T_N and T_c, respectively.

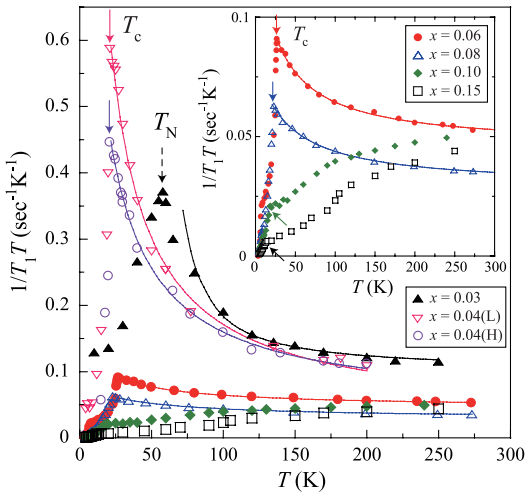

FIG. 3 (color online). T dependence of $1/T_1T$ for various x. The curves above T_N or T_c are fits to the AFSF theory (see the text). The inset is the enlarged part for $0.06 \leq x \leq 0.15$.

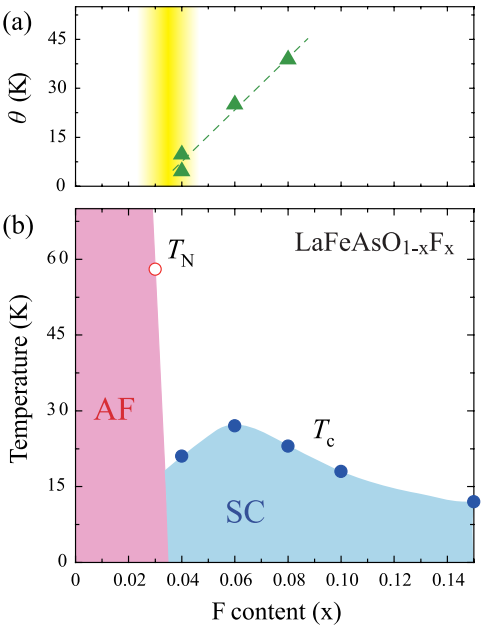

FIG. 4 (color online). Phase diagram obtained in this study. AF and SC denote the antiferromagnetically ordered and superconducting states, respectively. (a) x dependence of θ. The dotted line is a guide to the eyes. The shade indicates the region of phase separation. (b) x dependence of T_N and T_c determined by NQR measurements.

$\theta \sim 5$ K. The increase of θ with increasing x means that the system moves away from the magnetic instability (MI) where $\theta = 0$ K. With further doping, for $x = 0.10$ and 0.15, no enhancement of $1/T_1T$ is seen. Instead, $1/T_1T$ decreases with decreasing T, which was recently explained by the loss of the DOS due to a topological change of the Fermi surface [9,25]. The results in previous reports of the lack of the AFSF for $x \geq 0.10$ [12,13,15] are consistent with our results for $x = 0.10$ and 0.15.

The remarkable finding is that the highest $T_c = 27$ K is realized at $x = 0.06$, which is away from the MI. This situation is quite similar to the cuprates $La_{2-x}Sr_xCuO_4$ [26]. In the scenario of spin fluctuation-mediated superconductivity, this can be understood as follows. At high doping levels, the decrease of T_c is due to the weakening of the AFSF. In the vicinity of the MI, on the other hand, the too strong low-energy fluctuation acts as pair breaking [27]. Therefore, a maximal T_c is realized at some point away from the MI with moderate AFSF.

Figure 4 shows the phase diagram for $LaFeAsO_{1-x}F_x$ obtained in the present study. The most important finding is that the highest T_c is found in the low-doping regime, which makes our T_c vs x relation look like a dome shape. In the previous study [1,28], the failure of obtaining higher T_c in the low-doping regime is probably due to sample inhomogeneity as evidenced by the broader (in fact, two-peak-featured) NQR spectrum [29]. The present phase diagram is consistent with that for $Ba(Fe_{1-x}Co_x)_2As_2$ [7] but is somewhat different from that for $BaFe_2(As_{1-x}P_x)_2$ [10], whose T_c shows a maximum around $\theta = 0$. This slight difference may originate from the difference of the tuning parameter for their ground states. The ground states for both $LaFeAsO_{1-x}F_x$ and $Ba(Fe_{1-x}Co_x)_2As_2$ are tuned by electron doping. On the other hand, isovalent P doping acts as chemical pressure on $BaFe_2(As_{1-x}P_x)_2$. In any case, these phase diagrams support the intimate relationship between AFSF and superconductivity in iron arsenides. Furthermore, such a phase diagram has consistently been found in high-T_c cuprate $La_{2-x}Sr_xCuO_4$ [26] and heavy fermion compounds [30], indicating that the AFSF plays a significant role to induce superconductivity in strongly correlated electron systems in general.

Next, we turn to the superconducting state. Figure 5(a) shows the T dependence of $1/T_1$ for $x = 0.06$. Below T_c, $1/T_1$ decreases steeply due to the opening of the superconducting gaps. The hump structure at $T \sim 0.4T_c$ is due to the multiple-gap character as reported for other compounds [4–6,8]. The T variation at low T is much stronger than T^3 and even stronger than T^5, as can be clearly seen in the figure. In fact, $1/T_1$ decreases exponentially below $0.4T_c$. In Fig. 5(b), we plotted $1/T_1$ against T_c/T in a semilogarithmic scale. As indicated by the solid line, the $1/T_1$ below $T \sim 0.4T_c$ clearly follows the relation $1/T_1 \propto \exp(-\Delta_0/k_BT)$ with $\Delta_0/k_BT_c = 1.8$, where Δ_0 and k_B denote the gap size at $T = 0$ and the Boltzmann constant, respectively. This is clear and direct evidence that the superconducting state is fully gapped in $LaFeAsO_{0.94}F_{0.06}$.

The evolution of the superconducting-state properties can be seen in Fig. 2. For $x = 0.06$–0.10, $1/T_1$ shows a marked hump structure around $T \sim 0.4T_c$ and is followed by a still sharper decrease below. However, the low-T behavior of $1/T_1$ changes gradually, as to decrease less and less steeply as x increases. Eventually, for $x = 0.15$,

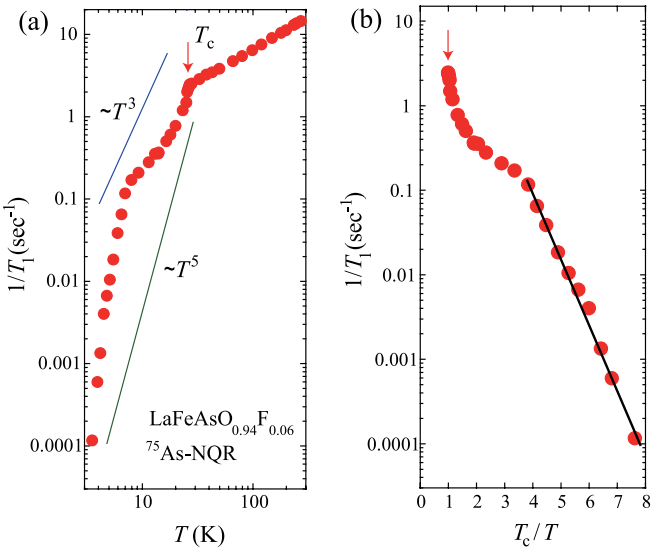

FIG. 5 (color online). (a) The T dependence of $1/T_1$ for $x = 0.06$. (b) Semilogarithmic plot of $1/T_1$ vs T_c/T. The solid line represents the relation $1/T_1 \propto \exp(-\frac{\Delta_0}{k_B T})$.

the hump structure disappears completely. Instead, a simple T dependence emerges which is close to T^3. Such T^3 behavior has been reported previously [12–14] and was taken as evidence for line nodes. Below, we show that it is a consequence of impurity scattering. Namely, the T^3 is an accidental one rather than an intrinsic one. In fact, in $Ba_{1-x}K_xFe_2As_2$, the low-T behavior of $1/T_1$ also changes when the sample purity differs [6,31].

Assuming sign reversing s-wave symmetry [32,33] with impurity scattering, one can reproduce the evolution of the $1/T_1$ below T_c. By introducing the impurity scattering parameter η in the energy spectrum in the form of $E = \omega + i\eta$, the $1/T_1$ in the superconducting state is given by $\frac{T_1(T_c)}{T_1(T)}\frac{T_c}{T} = \frac{1}{4T}\int_{-\infty}^{\infty}\frac{d\omega}{\cosh^2\frac{\omega}{2T}}(W_{\rm GG} + W_{\rm FF})$ [34], where $W_{\rm GG} = [\langle {\rm Re}\{(\omega + i\eta)/\sqrt{(\omega + i\eta)^2 + |\Delta(k_F)|^2}\}\rangle_{k_F}]^2$ and $W_{\rm FF} = [\langle {\rm Re}\{1/\sqrt{(\omega + i\eta)^2 + |\Delta(k_F)|^2}\}\Delta(k_F)\rangle_{k_F}]^2$. Here the Δ is the gap parameter, and $\langle \ldots \rangle$ is the average over the entire Fermi surface and runs over three bands consisting of two hole pockets at the Γ point and an electron pocket at the M point, respectively [35]. Namely, for a quantity F, $\langle F[\Delta(\mathbf{k}_F)]\rangle_{\mathbf{k}_F} = [N_1 F(\Delta_1^+) + N_2 F(\Delta_2^-) + N_3 F(\Delta_3^-)]/(N_1 + N_2 + N_3))$, where N_i is the DOS coming from band i ($i = 1, 2, 3$). Here, it is tempting to assign bands 1, 2, and 3 to the γ, β, and α bands found in angle-resolved photoemission spectroscopy measurement [36]. It is noted that the weaker T dependence in the $x = 0.15$ sample can be understood as due to the impurity scattering that brings about a finite DOS. For $x = 0.04$, where two As sites were found, $1/T_1$ for each site can also be fitted by the same model, with an additional feature that a large η is needed to explain the low-T behavior. This can be understood if the two phases coexist in the nanoscale

TABLE I. The fitting parameters $\Delta_1^+ (= \Delta_3^-)$, Δ_2^-, η in the unit of $k_B T_c$, and N_1:N_2:N_3.

x	T_c (K)	Δ_1^+	Δ_2^-	η	N_1:N_2:N_3
0.04(L)	21	4.50	0.93	0.39	0.335:0.330:0.335
0.04(H)	21	4.58	1.63	0.27	0.38:0.24:0.38
0.06	27	5.62	1.11	0.006	0.30:0.40:0.30
0.08	23	3.37	0.92	0.03	0.303:0.394:0.303
0.10	18	3.00	0.83	0.035	0.305:0.39:0.305
0.15	12	2.62	0.79	0.15	0.31:0.38:0.31

[22], where one phase acts as an impurity scatterer for the other. The obtained fitting parameters are summarized in Table I. Finally, we note that an s^{++} wave [37] seems difficult to explain the lack of the coherence peak just below T_c and the x evolution of low-T behavior of $1/T_1$.

In conclusion, we have presented the results of systematic NQR measurements on high quality samples of $LaFeAsO_{1-x}F_x$ ($x = 0.03$, 0.04, 0.06, 0.08, 0.10, and 0.15). The AFSF seen above $T_N = 58$ K of $x = 0.03$ persists in the $0.04 \leq x \leq 0.08$ regime. The highest $T_c = 27$ K is realized for $x = 0.06$, which is away from the magnetic instability but with significant AFSF. The phase diagram closely resembles those of the cuprates $La_{2-x}Sr_xCuO_4$ and other iron arsenides, which suggests that the AFSF is also important to produce the superconductivity in $LaFeAsO_{1-x}F_x$. In $x = 0.06$, $1/T_1$ below T_c decreases exponentially down to $0.13T_c$, which unambiguously indicates that the superconducting gaps are fully opened. The T variation of $1/T_1$ below T_c is rendered nonexponential for x either smaller or larger than 0.06, which is accounted for by impurity scattering.

We thank M. Ichioka for help in the calculation and K. Ishida for useful communication. Work in Okayama was supported in part by research grants from MEXT (No. 22103004 and No. 23102717). Work in Beijing was supported by CAS and NSFC.

[1] Y. Kamihara, T. Watanabe, M. Hirano, and H. Hosono, J. Am. Chem. Soc. **130**, 3296 (2008).
[2] X. H. Chen, T. Wu, G. Wu, R. H. Liu, H. Chen, and D. F. Fang, Nature (London) **453**, 761 (2008).
[3] Z.-A. Ren, W. Lu, J. Yang, W. Yi, X.-L. Shen, Z.-C. Li, G.-C. Che, X.-L. Dong, L.-L. Sun, F. Zhou, and Z.-X. Zhao, Chin. Phys. Lett. **25**, 2215 (2008).
[4] K. Matano, Z. A. Ren, X. L. Dong, L. L. Sun, Z. X. Zhao, and G.-q. Zheng, Europhys. Lett. **83**, 57 001 (2008).
[5] S. Kawasaki, K. Shimada, G. F. Chen, J. L. Luo, N. L. Wang, and G.-q. Zheng, Phys. Rev. B **78**, 220506(R) (2008).
[6] K. Matano, Z. Li, G. L. Sun, D. L. Sun, C. T. Lin, M. Ichioka, and G.-q. Zheng, Europhys. Lett. **87**, 27 012 (2009).

[7] F. L. Ning, K. Ahilan, T. Imai, A. S. Sefat, M. A. McGuire, B. C. Sales, D. Mandrus, P. Cheng, B. Shen, and H.-H. Wen, Phys. Rev. Lett. **104**, 037001 (2010).
[8] S. Kawasaki, T. Tabuchi, X. F. Wang, X. H. Chen, and G.-q. Zheng, Supercond. Sci. Technol. **23**, 054004 (2010).
[9] T. Tabuchi, Z. Li, T. Oka, G. F. Chen, S. Kawasaki, J. L. Luo, N. L. Wang, and G.-q. Zheng, Phys. Rev. B **81**, 140509(R) (2010).
[10] Y. Nakai, T. Iye, S. Kitagawa, K. Ishida, H. Ikeda, S. Kasahara, H. Shishido, T. Shibauchi, Y. Matsuda, and T. Terashima, Phys. Rev. Lett. **105**, 107003 (2010).
[11] H. Kinouchi, H. Mukuda, M. Yashima, Y. Kitaoka, P. M. Shirage, H. Eisaki, and A. Iyo, Phys. Rev. Lett. **107**, 047002 (2011).
[12] Y. Nakai, K. Ishida, Y. Kamihara, M. Hirano, and H. Hosono, J. Phys. Soc. Jpn. **77**, 073701 (2008).
[13] H.-J. Grafe, D. Paar, G. Lang, N. J. Curro, G. Behr, J. Werner, J. Hamann-Borrero, C. Hess, N. Leps, R. Klingeler, and B. Büchner, Phys. Rev. Lett. **101**, 047003 (2008).
[14] H. Mukuda, N. Terasaki, H. Kinouchi, M. Yashima, Y. Kitaoka, S. Suzuki, S. Miyasaka, S. Tajima, K. Miyazawa, P. Shirage, H. Kito, H. Eisaki, and A. Iyo, J. Phys. Soc. Jpn. **77**, 093704 (2008).
[15] Y. Nakai, S. Kitagawa, K. Ishida, Y. Kamihara, M. Hirano, and H. Hosono, New J. Phys. **11**, 045004 (2009).
[16] Y. Kobayashi, E. Satomi, S. C. Lee, and M. Sato, J. Phys. Soc. Jpn. **79**, 093709 (2010).
[17] C. Martin, M. E. Tillman, H. Kim, M. A. Tanatar, S. K. Kim, A. Kreyssig, R. T. Gordon, M. D. Vannette, S. Nandi, V. G. Kogan, S. L. Budko, P. C. Canfield, A. I. Goldman, and R. Prozorov, Phys. Rev. Lett. **102**, 247002 (2009).
[18] T. Sato, S. Souma, K. Nakayama, K. Terashima, K. Sugawara, T. Takahashi, Y. Kamihara, M. Hirano, and H. Hosono, J. Phys. Soc. Jpn. **77**, 063708 (2008).
[19] R. S. Gonnelli, D. Daghero, M. Tortello, G. A. Ummarino, V. A. Stepanov, R. K. Kremer, J. S. Kim, N. D. Zhigadlo, and J. Karpinski, Physica (Amsterdam) **469C**, 512 (2009).
[20] G. F. Chen, Z. Li, G. Li, J. Zhou, D. Wu, J. Dong, W. Z. Hu, P. Zheng, Z. J. Chen, H. Q. Yuan, J. Singleton, J. L. Luo, and N. L. Wang, Phys. Rev. Lett. **101**, 057007 (2008).
[21] See Supplemental Material at http://link.aps.org/supplemental/10.1103/PhysRevLett.108.047001 for details on sample quality and x dependence of ν_Q.
[22] G. Lang, H.-J. Grafe, D. Paar, F. Hammerath, K. Manthey, G. Behr, J. Werner, and B. Büchner, Phys. Rev. Lett. **104**, 097001 (2010).
[23] T. Moriya, *Spin Fluctuations in Itinerant Magnetism* (Springer, Berlin, 1985).
[24] The deviation may be understood as due to impurity scattering by another phase that coexists in the nanoscale [22].
[25] H. Ikeda, R. Arita, and J. Kuneš, Phys. Rev. B **82**, 024508 (2010).
[26] S. Ohsugi, Y. Kitaoka, K. Ishida, G.-q. Zheng, and K. Asayama, J. Phys. Soc. Jpn. **63**, 700 (1994).
[27] T. Moriya and K. Ueda, J. Phys. Soc. Jpn. **63**, 1871 (1994).
[28] H. Luetkens, H.-H. Klauss, M. Kraken, F. J. Litterst, T. Dellmann, R. Klingeler, C. Hess, R. Khasanov, A. Amato, C. Baines, M. Kosmala, O. J. Schumann, M. Braden, J. Hamann-Borrero, N. Leps, A. Kondrat, G. Behr, J. Werner, and B. Büchner, Nature Mater. **8**, 305 (2009).
[29] S. Kitagawa, Y. Nakai, T. Iye, K. Ishida, Y. Kamihara, M. Hirano, and H. Hosono, Physica (Amsterdam) **470C**, S282 (2010).
[30] N. D. Mathur, F. M. Grosche, S. R. Julian, I. R. Walker, D. M. Freye, R. K. W. Haselwimmer, and G. G. Lonzarich, Nature (London) **394**, 39 (1998).
[31] Z. Li, D. L. Sun, C. T. Lin, Y. H. Su, J. P. Hu, and G.-q. Zheng, Phys. Rev. B **83**, 140506(R) (2011).
[32] I. I. Mazin, D. J. Singh, M. D. Johannes, and M. H. Du, Phys. Rev. Lett. **101**, 057003 (2008).
[33] K. Kuroki, S. Onari, R. Arita, H. Usui, Y. Tanaka, H. Kontani, and H. Aoki, Phys. Rev. Lett. **101**, 087004 (2008).
[34] Z. Li, Y. Ooe, X. C. Wang, Q. Q. Liu, C. Q. Jin, M. Ichioka, and G.-q. Zheng, J. Phys. Soc. Jpn. **79**, 083702 (2010).
[35] D. J. Singh and M. H. Du, Phys. Rev. Lett. **100**, 237003 (2008).
[36] H. Ding, P. Richard, K. Nakayama, K. Sugawara, T. Arakane, Y. Sekiba, A. Takayama, S. Souma, T. Sato, T. Takahashi, Z. Wang, X. Dai, Z. Fang, G. F. Chen, J. L. Luo, and N. L. Wang, Europhys. Lett. **83**, 47 001 (2008).
[37] H. Kontani and S. Onari, Phys. Rev. Lett. **104**, 157001 (2010).